Spread spectrum time- and space-integrating optical processor

Demetri Psaltis and David Casasent

A hybrid time- and space-integrating optical signal processor for spread spectrum application is described. The system is self-synchronizing and capable of decoding frequency-hopped spread spectrum signals with a large time–bandwidth product. Extensions to hybrid frequency-hopped/direct-sequence systems and to ambiguity function processors are provided. Both theory and experimental verification are included.

I. Introduction

Spread spectrum (SS) systems[1] are well known to provide high processing gain and noise jammer immunity. These features are necessary in advanced communications, radar, and C^{3}I systems.[2] The bandwidth and time–bandwidth product (TBW) of the codes under consideration in advanced SS systems are increasing so rapidly that they threaten to exceed our ability to process accurately such data in real time. For these reasons, optical signal processors have recently received renewed attention.[3] This research has been fostered by recent advances in acoustooptic (AO) transducers, novel signal processing architectures, and new signal processing algorithms.[3]

The SS system we consider uses a frequency-hopped (FH) code. Self-synchronization and decoding of the data with a large delay range search window and long TBW codes are the processor features we desire. In Sec. II we define the SS signal processing required. The optical processor is then described in Sec. III. Experimental verification is included in Sec. IV.

The authors are with Carnegie-Mellon University, Department of Electrical Engineering, Pittsburgh, Pennsylvania 15213.

Received 3 November 1979.
0003-6935/80/091546-04$00.50/0.

II. FH SS Signal Processing Theory

A specific formulation of the signal processing requirements for a FH SS system is provided that best enables the optical signal processing architecture to be described. We describe the FH SS transmitted signal as follows:

$$a(t) = \sum_{m}^{M} \Pi\left[\frac{t - (m + \tfrac{1}{2})t_0}{t_0}\right] \exp(j2\pi f_m t), \tag{1}$$

where

$$\Pi\left(\frac{t-a}{b}\right) = 1 \text{ for } a - b/2 \leq t \leq a + b/2, \text{ zero otherwise.} \tag{2}$$

This describes a sequence of M frequencies f_m, each of chirp duration t_0, centered at $t = (m + \tfrac{1}{2})t_0$. The summation describes the sequence of different frequencies used in the different t_0 time slots. The frequency sequence $\{f_m\} = f_1 \ldots f_m \ldots f_M$ does not imply a linear sequence of frequencies, i.e., $f_3 > f_2 > f_1$, etc.

The received signal $b(t)$ is a delayed version of $a(t)$ described by Eq. (1) with $m = n$. In most cases, the cross correlation of $a(t)$ and $b(t)$ is performed. In a radar SS system, the range and often Doppler of the target is estimated by the position of the correlation peak. In a SS communication system, the data are encoded in the polarity of the correlation peak. In both cases, a matched spatial filter (MSF) correlation processor is optimum for detection of a signal in white noise.[4] For FH systems, the MSF produces approximately the optimum processing gain ($M - 1$ vs M). In all the cases to be considered, we assume use of a moving window time domain optical correlator that realizes the cross correlation as

$$R(t) = \int a(\tau)b^*(\tau - t)d\tau$$

$$= \sum_n^M \exp(j2\pi f_n t) \sum_m^M \int_{-\infty}^{\infty} \exp[j2\pi(f_m - f_n)\tau]\Pi\left[\frac{\tau - (m + \tfrac{1}{2})t_0}{t_0}\right]\Pi\left[\frac{\tau - t - (n + \tfrac{1}{2})t_0}{t_0}\right]d\tau. \quad (3)$$

This type of correlator enables us to search the desired large range delay. If $f_m \neq f_n$, a beat frequency that is an integer multiple of the step frequency $\Delta f = \min(f_m - f_n)$ results. If the instantaneous bandwidth $1/t_0$ of the transmitted data is less than Δf, the integral in Eq. (3) approaches 0, and thus the correlation integral in Eq. (3) has a value only for $f_m = f_n$. For $\Delta f > 1/t_0$, Eq. (3) reduces to

$$R(t) = \sum_m^M \exp(j2\pi f_m t) \int_{-\infty}^{\infty} \Pi\left[\frac{\tau - (m + \tfrac{1}{2})t_0}{t_0}\right] \times \Pi\left[\frac{\tau - t - (m + \tfrac{1}{2})t_0}{t_0}\right]d\tau. \quad (4)$$

Anticipating the method by which the correlation in Eq. (3) will be realized by formation of the Fourier transform of $b(t)$ in an AO processor, we write the corresponding input signal as $b(t - \tau')\Pi(\tau'/t_0)$, where $\tau' = x/v$, x is the spatial AO line variable and also the shift variable with units of time that correspond to spatial distance. The Fourier transform with respect to τ' of this signal is a function of time and frequency:

$$F(t,f) = \exp(-j2\pi ft) \sum_m^M \int_{-\infty}^{\infty} \Pi\left(\frac{t - \tau}{t_0}\right)\Pi\left[\frac{\tau - (m + \tfrac{1}{2})t_0}{t_0}\right]\exp(j2\pi f_m\tau)\exp(j2\pi f\tau)d\tau, \quad (5)$$

where the variable substitution $t - \tau' = \tau$ or $\tau' = t - \tau$ has been used, and the expression from Eq. (1) has been substituted for $b(t)$ with constant factors omitted. Comparing Eqs. (4) and (5) and realizing that the first exponential term in Eq. (4) is of no concern when $|R|^2$ is measured (because it integrates out as described above), we note that $R(t)$ can be obtained by the following three steps:

(1) Formation of the Fourier transform $F(t,f)$ over a time window t_0 of the received signal $b(t)$. Note that this Fourier transform varies with time and frequency (or space).

(2) Evaluation or sampling of $F(t,f)$ at $f = -f_m$. For each $f = -f_m$, the Fourier transform varies as a function of time.

(3) Delaying $F(t,f_m)$ by $(m + \tfrac{1}{2})t_0$ for each f_m and summing the selected and delayed specifically evaluated Fourier transforms over all the values of m.

We thus describe our self-synchronizing and decoding algorithm to obtain $R(\tau)$ from $F(t,f)$ as

$$\left|R(t)\right|^2 = \sum_m^M \left|F[t + (m + \tfrac{1}{2})t_0, -f_m]\right|^2. \quad (6)$$

III. Optical Processor for FH SS Data

The optical signal processor in Fig. 1 performs the required processing to produce $R(\tau)$ in Eq. (3) for all the range delays using the algorithm described above. The received signal $b(t)$ is fed to the AO cell at P_1. Its transmittance is $b(t - \tau')\Pi(\tau'/t_0)$. The 1-D horizontal Fourier transform of this signal, described by Eq. (5), is incident on P_2. This Fourier transform pattern is a function of time and frequency (or space) as noted in Eq. (5). A mask is placed at P_2 with slits at horizontal locations corresponding to the frequencies f_m in the code. The sequence of FH frequencies $\{f_m\}$ is encoded by the ordered sequence of the vertical locations of the apertures at P_2. The P_2 mask thus has axes f_m (horizontal) and m (vertical). P_2 is imaged vertically to image each frequency band onto one detector and demagnified horizontally to collect all the light from each band onto a vertical linear detector array at P_3. At $t = t_0$, f_1 is present, and detector element 1 (the top detector element) receives a pulse of light. At $t = 2t_0$, f_2 is present in the input. The aperture at the corresponding vertical location in row 2 in P_2 now transmits light; this is incident on detector 2 in the output, and this process continues.

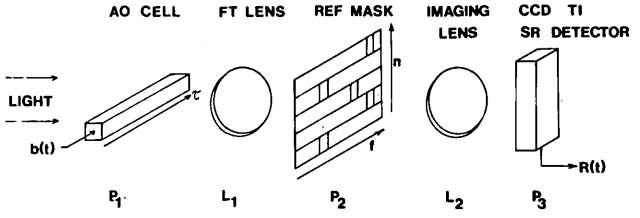

Fig. 1. Schematic diagram of an optical hybrid time- and space-integrating spread spectrum processor.

When the output detector array is an integrating CCD shift register,[7] the detected CCD outputs are integrated during the chip duration t_0 and the shifted down vertically at a clock rate equal to $1/t_0$. Thus, after Mt_0, the Mth CCD detector contains the summation over m of M frequency pulses, all with the proper time delay and in the proper coded frequency sequence. Thus the optical system of Fig. 1 provides the correlation of a long time duration signal of M chips with a wide signal bandwidth and yet with a long range delay search window. By performing the processing of the signal in M parts, each of low time duration t_0, and properly summing each output, a large TBW correlation is achieved. The resultant optical processor is a time- and space-integrating correlator (a TSI system). The space integration[5] is performed by the Fourier transform lens over space τ, and the time integration[6] is

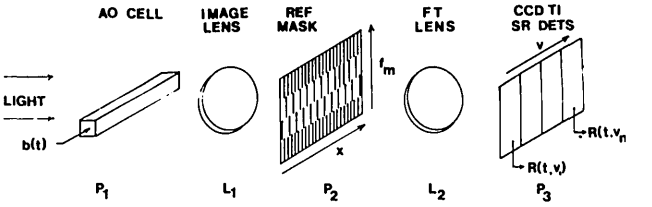

Fig. 2. Schematic diagram of an optical hybrid time- and space-integrating ambiguity function spread spectrum processor.

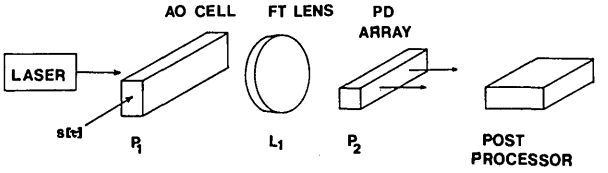

Fig. 3. Schematic diagram of the experimental optical spread spectrum processor.

performed by properly delaying and summing the output signal at different instances in time over m (this is achieved by the vertical location of the slits in the optical mask at P_2 and by the choice of the clock rate for the output CCD shift register detector).

In the design of this system, we chose the output detector shift rate to be $1/t_0$ and the aperture time of the input AO cell to be t_0 also. In terms of Eq. (5) the Fourier transform is performed by L_1 on the AO line data at P_1. The sampling and evaluation of Eq. (5) at f_m are performed by the vertical slits in the mask at P_2; the time delay and summation of these outputs are achieved by the choice of the vertical locations of the apertures in P_2, the clock rate $1/t_0$ of the output CCD detector, and the aperture time t_0 of the input AO cell. The output correlation SNR obtained is within 3 dB of the optimum due to the noncoherent summation in Eq. (5). The full optimum output SNR can be obtained by varying the clock rate of the output detector or the synchronization rate of a pulse input laser source. The sync rate of the detector need only be varied over a $t_0/2$ delay time to be phase locked to the signal and achieve optimum system correlation performance. In the most simplified description of this system, we can view it as an optically addressed electronic correlator (the CCD shift register detector) in which the optical system is used to present the necessary inputs to the electronic filter in the correct time and space format.

This system can easily be modified for single sideband modulation and decoding of information. In such a case, complementary frequency encoding is used. In such modulation, a set of M frequencies $\{f_m\}$ are chosen for the FH code. One-half of the frequencies are used to transmit a 1, and the other half to transmit a 0. The two sets of frequencies are complements with respect to the carrier center frequency f_0, i.e., we describe one FH set of frequencies by

$$\sum_m \exp[j2\pi(f_0 + f_m)]$$

and the other set by

$$\sum_m \exp[j2\pi(f_0 - f_m)].$$

To decode such complementary frequency encoded FH data, we must evaluate the Fourier transform of $b(t)$ at $\pm f_m$ rather than at just $-f_m$, evaluate the 1 and 0 FH sequences as in Fig. 1, and detect the two possible outputs on two linear output detector arrays as above. Since a coherent optical system automatically forms both the $\pm f_m$ frequencies, this decoding scheme with the indicated complementary frequency FH coding is thus directly realizable on the same optical system. The processing gain of this system will equal the number of detector elements ($>10^3$ with state-of-the-art components).

Extensions of the basic system to hybrid FH/DS coding schemes, in which a DS or PRN code of M chips is transmitted at each of the f_m frequencies in the FH code, are also possible. In this case, synchronization is easily possible only over the DS code length.

As the final extension of this TSI system, we consider a SS radar application in which a Doppler shift can occur between the transmitted and received signals. In this case, the range delay and Doppler shift are desired, i.e., an ambiguity function output display.[4] The system of Fig. 2 achieves this. The input signal $b(t - \tau')\Pi(\tau'/t_0)$ is now imaged onto a mask at P_2, consisting of gratings at spatial frequencies corresponding to frequencies $\{f_m\}$ in the FH code ordered vertically in the frequency sequence of the code. The vertical magnification between P_1 and P_2 is such that the image of P_1 illuminates all the frequency channels at P_2 simultaneously. We assume a constant Doppler shift over the

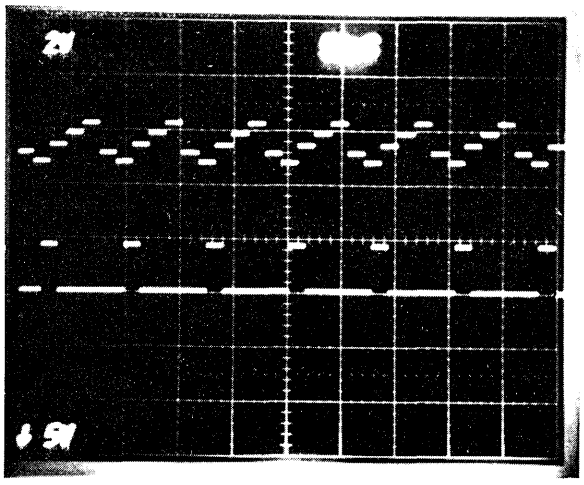

Fig. 4. (a) Input and (b) output from the optical spread spectrum processor of Fig. 3.

code length that is small compared with f_m. Multiplication of $b(t)$ by the P_2 mask produces a beat frequency equal to the difference between the received and transmitted frequencies. The Fourier transform performed by L_2 causes the output Fourier transform to deflect horizontally proportional to this beat frequency or Doppler shift. At P_3, a 2-D vertical linear detector array is placed. The proper ordering of the mask's spatial frequencies together with the time-integrating shift register output CCD detector provide the desired $R(t)$ output vertically as before. The linear vertical detector array in the 2-D output plane on which the output occurs yields the necessary Doppler information. The entire 2-D output is the ambiguity function.

Thus, the basic optical signal processor of Fig. 1 can provide synchronization and correlation of a FH sequence with long input time duration Mt_0 (msec or more) and large overall bandwidths M/t_0 (10^8–10^9 Hz or more) with modest individual component specifications. This is achieved by the TSI system described in which a space-integrating Fourier transform system produces a time varying signal spectrum, which is then integrated in time over the output detector.

IV. Experimental Conformation

To demonstrate the basic principle of operation of the SS optical signal processor described in Sec. III, the system of Fig. 3 was assembled. For the experiments performed the chip length was $t_0 = 1/60$ kHz = 16 μsec (equal to the aperture time of the AO cell at P_1 of Fig. 3), the set of five frequencies used was $\{f_i\} = f_1 \ldots f_5$, where $f_1 = 32$ MHz and $\Delta f = 1.2$ MHz, and the FH code chosen was $\{f_m\} = f_2, f_1, f_3, f_4$, and f_5.

Because a shift, delay, and integrating CCD output detector array of the type necessary was not available to us, the necessary sum and delay operations were performed in special purpose postdetector hardware using amplifiers, threshold detectors, flip-flops and adders properly hardwired to the correct detector outputs for the FH code used. In Fig. 4(a), the voltage controlled oscillator input to the AO cell (frequency vs time) is shown for seven cycles of the code. The resultant output from the digital postprocessor is shown in Fig. 4(b). As predicted, an output correlation peak occurs whenever the correct input code is present, and the time of occurrence of the output peak indicates the range delay between the received and transmitted signals. The system was also tested with other FH code inputs to demonstrate its ability to discriminate in a multiuser application (excellent results occurred as predicted by theory). The performance of the system in the presence of a single frequency jammer at one of the frequencies $\{f_i\}$ was also tested. In this case, an output analogous to the one in Fig. 4(b) was obtained with the output dc level increased by one part in M, where M is the number of frequencies in the FH code. This is in agreement with theory and demonstrates the processing gain and use of the system in practical noise environments.

The support of the National Science Foundation and motivation by Hanscom Air Force Base for this research are gratefully acknowledged. The authors also thank M. Libby for performing the experiments noted in Sec. IV and M. Gottlieb and F. Caimi for assistance in the fabrication and design of the transducer and its support systems.

References

1. R. C. Dixon, *Spread Spectrum Systems* (Wiley, New York, 1976).
2. Proc. Soc. Photo-Opt. Instrum. Eng. **204**, Oct. (1979).
3. Proc. Soc. Photo-Opt. Instrum. Eng. **154** (1978); **180** (1979); **185** (1979); **202** (1979).
4. A. W. Rihaczek, *Principles of High Resolution Radar* (McGraw-Hill, New York, 1969).
5. L. Cutrona *et al.*, IRE Trans. Inf. Theory **IT-6**, 386 (1960).
6. R. Sprague and C. Koliopoulos, Appl. Opt. **15**, 89 (1976).
7. M. Monahan *et al.*, IOCC Conf., Apr. 1975, IEEE Cat. No. 75-CH0941-5C, p. 25.